

Evaluation of the comparative effects of infrared and red laser photobiomodulation therapy on skeletal muscle atrophy in an immobilization model in rats

Silma Rodrigues Gonçalves¹, Carla Roberta Tim¹, Nivaldo Antonio Parizotto¹, Cintia Cristina Santi Martignago², Marcelo Cavenaghi Pereira da Silva³, Carlos Alberto Anaruma⁴, Hananiah Tardivo Quintana⁴, Livia Assis¹

¹Pós-Graduação em Engenharia Biomédica, Instituto Científico e Tecnológico, Universidade Brasil (UB) - São Paulo (SP), Brazil

²Universidade Federal de São Paulo (UNIFESP) – Santos (SP), Brazil

³Departamento de Morfologia, Universidade Federal de São Paulo (UNIFESP) - São Paulo (SP), Brazil

⁴Departamento de Educação Física, Universidade Estadual Paulista (UNESP) - Rio Claro (SP), Brazil

ABSTRACT

Introduction: Skeletal muscle atrophy leads to a reduction in muscle strength, functionality, and the quality of life of individuals. **Objective:** To explore the effects of two different wavelengths (red and infrared) of laser PBMT on muscle atrophy and its active ingredients on skeletal muscle atrophy using an in vivo model of muscle atrophy. **Methods:** Thirty-two Wistar rats were randomly divided into four experimental groups: control (CG) animals were not immobilized and did not receive any type of treatment; immobilized animals with no treatment (ImC); immobilized animals submitted to red laser with wavelength of 660 nm (ImR) and near-infrared laser with wavelength of 808 nm (ImIR) treatments. The treatments were applied daily, at 2 points in the right gastrocnemius muscle (cranial and caudal), through the punctual contact technique, for 9 sessions, with the first application immediately after removing the cast. **Results:** The histological results demonstrated that in both treated groups (red and infrared wavelengths) a reduction of the inflammatory infiltrate and less connective tissue thickening when compared to the ImC. However, only infrared light was observed regenerating muscle fibers and an increase in the number of oxidative fibers (type I). **Conclusion:** These results suggest that red and infrared wavelength laser PBMT were able to promote changes in the morphology of the gastrocnemius muscle submitted to atrophy in an experimental immobilization model, reducing the inflammatory infiltrate and the formation of intramuscular connective tissue. However, infrared laser PBMT promoted more evident positive effects by increasing regenerating muscle fibers and the number of oxidative fibers.

Keywords: phototherapy; low-level laser therapy; muscular atrophy; immobilization.

INTRODUCTION

The loss of muscle mass or skeletal muscle atrophy can be clinically detected in the elderly, in situations of disuse and prolonged immobilization, and in various clinical conditions such as cancer, diabetes mellitus, heart and lung diseases, acquired

How to cite this article: Gonçalves et al. Evaluation of the comparative effects of infrared and red laser photobiomodulation therapy on skeletal muscle atrophy in an immobilization model in rats. *ABCS Health Sci.* 2023;48:e023232 <https://doi.org/10.7322/abcshs.2021248.1964>

Received: Nov 03, 2021

Revised: Mar 03, 2022

Approved: Apr 01, 2022

Corresponding author: Livia Assis - Pós-Graduação em Engenharia Biomédica, Instituto Científico e Tecnológico, Universidade Brasil - Rua Carolina Fonseca, 584 - CEP: 08230-030 - Itaquera (SP), Brazil - E-mail: livinha_fisio@yahoo.com.br

Declaration of interests: nothing to declare
Funding: CAPES



This is an open access article distributed under the terms of the Creative Commons Attribution License
© 2023 The authors

immunodeficiency syndrome (HIV), sepsis, denervation, muscular dystrophies and in the 2019 coronavirus disease (COVID-19) caused by the coronavirus 2 (SARS-CoV-2)¹⁻⁴.

It is estimated that this type of musculoskeletal change has increased by 46% in recent years due to population aging and prolonged hospitalization. Functional outcomes are heterogeneous while some individuals fully recover, others will remain with persistent muscle weakness. Sustained muscle atrophy follows in functional limitations, and decreased quality of life⁵⁻⁸. In this sense, research aimed at developing therapeutic interventions aimed at attenuating the atrophy process, stimulating the regenerative process, as well as favoring the structural and functional recovery of muscle tissue is extremely important.

Currently, photobiomodulation therapy (PBMT) using lasers (light amplification by stimulated light emission) and LEDs (light emitting diodes) has been identified as a safe and promising tool for the treatment of a variety of diseases and musculoskeletal injuries because it has modulating properties of the inflammatory, analgesic and repairing process⁹.

It is known that monochromatic light penetrates tissues and is absorbed by specific cellular photoreceptors, called chromophores, promoting various cellular and molecular modifications^{10,11}, as an increase in mitochondrial membrane potential and synthesis of adenosine triphosphate (ATP), stimulating the transcription of several genes responsible for increasing the endogenous antioxidant defense system, preventing and repairing muscle damage, as well as optimizing the performance of muscle fibers¹²⁻¹⁴.

Lakyová et al.¹⁴ observed that red wavelength laser caused a profound reduction in muscle atrophy and enhanced recovery after the ischemia/reperfusion muscle atrophy model in rats by attenuating the inflammatory reaction and facilitating angiogenesis. Although some studies are showing the positive effect of laser PBMT on changes in skeletal muscle tissue, some issues regarding muscle atrophy in immobilization are not yet known. There are few studies in the literature investigating the effect of different laser PBMT wavelengths in the treatment of muscle atrophy.

In this context, it was hypothesized that laser PBMT could influence cell metabolism, increasing tissue bioenergetics, and attenuating the muscle proteolysis process, constituting an adequate and effective treatment to be used in clinical practice. In this sense, cellular evidence in this scenario would be of great value to accurately understand the benefits of using these therapeutic approaches in muscle tissue recovery after muscle atrophy, particularly because evidence is scarce in this area of knowledge.

Using an experimental model of muscle atrophy by plastered immobilization, a study focused on evaluating the effects of PBMT on the red and infrared wavelengths through histopathological and histochemical analysis of muscle tissue was carried out.

METHODS

Experimental Design

The Ethics Committee on the Use of Animals of the UNESP (São Paulo State University) approved this research (CEUA protocol 5937). Thirty-two male Wistar rats were used (male, *Rattus norvegicus* Albinus, Rodentia, Mammalia, average body mass of 250 g), remained in collective polypropylene cages, transparent, with one animal per cage, under controlled humidity and temperature (23°-25°C), 12 hours dark/light cycle, with free access to balanced food and filtered water.

Rats were divided into 4 groups (n=8 each): basal control (CG) animals were not immobilized and did not receive any type of treatment; immobilized animals with no treatment (ImC); immobilized animals submitted to red laser with a wavelength of 660 nm treatment (ImR); immobilized animals submitted to near-infrared laser with a wavelength of 808 nm treatment (ImIR).

Experimental muscle atrophy induction

Rats were anesthetized before the wound induction, with an intraperitoneal injection of ketamine and xylazine (doses of 40 and 10 mg/kg, respectively – Vetbrands, Brazil) and then their hind limbs were trichotomized. Subsequently, a monolateral immobilization of the right hind limb was performed for each animal using a plaster cast splint with full plantar extension for 5 days. The mold was wrapped with a fine mesh steel mesh to prevent chewing according to Aoki et al.¹⁵. At the end of the procedure, the animals received appropriate post-anaesthesia care.

PBMT Protocol

A gallium-aluminium-arsenide (GaAlAs) diode laser (Photon Laser II, DMC® equipment Ltda, SP, São Carlos, Brazil), was used in the following parameters: continuous irradiation mode, 808 nm wavelength, 30 mW power output, 56 sec irradiation time, 0.028 cm² spot area, dose 60 J/cm², irradiance 1.07 W/cm², 1.4 J total energy per point/section. The PBMT irradiation was performed daily for nine consecutive days, starting immediately after removing the cast at 2 points: right gastrocnemius muscle (cranial and caudal), through the punctual contact technique. Ten days after surgery, all animals were euthanized individually by anesthesia overdose (twofold anesthesia dose), and the muscle of each animal was removed for analysis.

Histopathological analysis

After the euthanasia of the animals, the right gastrocnemius muscle was collected. The muscle was immediately frozen in isopentane pre-cooled in liquid nitrogen, and then stored in a freezer at -80 °C (Forma Scientific, Marietta, OH). Serial muscle cross-sections for histology were obtained (one section of 10 µm in each 100 µm of tissue) using a cryostat microtome (Micron HE

505, Jena, Germany). Five sections of each specimen were stained with hematoxylin and eosin (HE stain, Merck), and the other five sections were submitted to Histochemistry of myosin ATPase and examined using light microscopy (Leica Microsystems AG, Wetzlar, Germany) and five sections of each specimen were submitted to Histochemistry of myosin ATPase.

Muscle fiber cross-sectional area (CSA) and muscle fiber density analysis

The CSA and muscle fiber density were examined under light microscopy (Leica Microsystems AG, Wetzlar, Germany), with a 4x objective, using a computer-based image analysis technique (AxioVision 4.7; Carl Zeiss, Oberkochen, Germany). The CSA and the number of fibers were obtained by measuring the area of fibers located in six preselected ($150 \mu\text{m}^2$) areas. A double-blind procedure (LA and SG) was used for measurements¹⁵.

Histochemistry of myosin ATPase

The muscle-type fibers were identified through the myosin ATPase reaction was used to identify. ATP is the reaction energy source, myosin is the enzyme, and substrate Pi is the reaction product. The Pi is not visible by histochemistry, the reaction requires that Pi react with calcium to form the precipitate calcium phosphate. The next step in the process produces brownish black cobalt sulfide, easily visible and less soluble. As Pi is released by the myosin molecule's consumption of ATP, a brownish-black product is deposited on the muscle tissue section. The fast-contracting fibers appear dark histochemical, and the slow-contracting fibers appear light. Type I fibers react deeply after acid preincubation at pH 4.3, and lightly after alkali pre-incubation at pH 10.3. The opposite occurs with type II muscle fibers¹⁶. The density of type I and II fibers was evaluated in six preselected areas ($150 \mu\text{m}^2$), under a light microscopy, with a 4x objective.

Statistical Analysis

The 6.01 GraphPad Software (USA) was used for statistical analysis. The data were submitted to the Shapiro-Wilk's normality test. How the resulting data had no normal distribution, they were statistically analyzed by using the Kruskal-Wallis test followed by Dunn's test. The significance level of 5% ($p \leq 0.05$) was considered.

RESULTS

Histological descriptive analysis

Representative images of the gastrocnemius muscle sections are shown in Figure 1. Histopathological analysis revealed that the CG group had normal skeletal striated muscle tissue structures, exhibiting muscle fibers with regular polygonal aspect, homogeneous size, peripheral nuclei, and organization fibers

equidistant from each other and in normal fascicular distribution. For the immobilized animals (ImC, ImR, and ImIR), morphological changes were observed, including muscle fibers with varied shapes and irregular size, infiltration of undifferentiated cells (inflammatory), and thickening of the intramuscular connective tissue more evident in the perimysium. The groups treated with laser PBMT (ImR and ImIR) had similar histological findings, with a reduced amount of inflammatory cell infiltrate and less connective tissue thickening when compared to immobilized animals that did not receive treatment. These changes were more evident in the ImIR group, which presented reduced inflammatory infiltrate, and mild connective tissue thickening, and it was possible to observe muscle fibers with a central nucleus, which resemble regenerating fibers, when compared to the ImR group.

Morphometry of CSA

Figure 2 illustrates the data obtained for CSA evaluation. A significant reduction in muscle fiber CSA was observed in the ImC group ($p=0.0131$), ImR ($p=0.0285$), and ImIR ($p=0.0019$) when compared to the CG group. No other statistical differences were observed between the other experimental groups.

Muscle Fiber Density

The values obtained in the muscle fiber density analysis can be observed in Figure 3. Muscle fiber density analysis revealed that all immobilized groups, ImC ($p=0.002$), ImR ($p=0.0156$), and ImIR ($p=0.0017$) produced a significant increase in fiber density compared with the CG. No other statistical differences were observed between the other experimental groups.

ATPase descriptive analysis

Figure 4 reveals the morphological evaluation of type I and II muscle fibers. In group CG it is possible to identify type I and type II fibers. However, in the immobilized groups, type II fibers are predominant compared to the CG. No other differences were observed between the immobilized groups.

Type I fiber density analysis

The density of type I fiber evaluation (Figure 5) exhibited a reduction in the immobilized experimental groups ImC ($p=0.002$) and ImR (0.003) when compared to the CG group. Furthermore, an increase in the density of type I fibers was observed in the ImIR group compared to the ImC ($p=0.002$) and ImR ($p=0.029$) groups.

Type II fiber density analysis

Figure 6 shows the morphometric evaluation of type II fiber density. It was possible to verify an increase in all immobilized groups (ImC, ImR, and ImIR) compared to the CG group. No additional differences were observed.

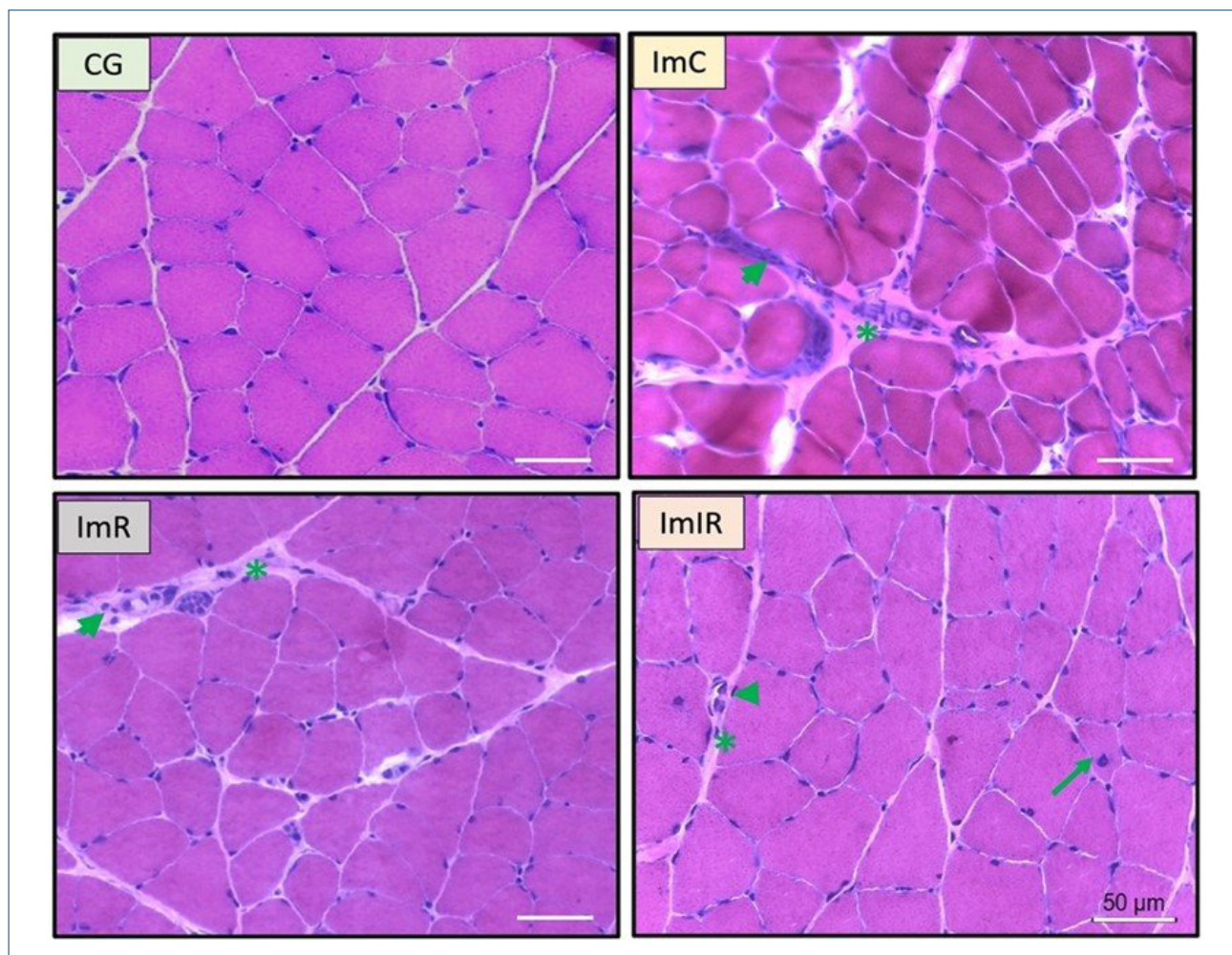


Figure 1: Photomicrographs of morphological analysis of gastrocnemius muscle cross-sections. Normal fibers (arrowhead); connective tissue (asterisks), inflammatory infiltrate (arrowhead); fiber with central nucleus (arrow). Basal control (CG) animals were not immobilized and did not receive any type of treatment; immobilized animals with no treatment (ImC); immobilized animals submitted to red laser with a wavelength of 660 nm treatment (ImR); immobilized animals submitted to near-infrared laser with a wavelength of 808 nm treatment (ImIR). (Stain: HE; Scale bar: 50 µm).

DISCUSSION

Considering the need to provide subsidies for the implementation of more specific and targeted intervention plans for the rehabilitation of patients with muscle atrophy, this study was conducted. The main results show that laser treatment with PBMT at both wavelengths was able to reduce the inflammatory infiltrate and the amount of intramuscular connective tissue. It is noteworthy that these findings were more pronounced in the ImIR group, and it is possible to observe morphological findings of regenerating muscle fibers and an increase in the number of oxidative fibers (type I fibers) when compared to the other immobilized groups.

As previously described, muscle atrophy remains a prevalent clinical challenge and the methods used for rehabilitation are often still poorly understood^{5,6}. To investigate the complex cellular and molecular mechanisms triggered by different types of treatments, animal models have been used, with the

immobilization technique being the most frequently used for inducing muscle atrophy¹⁷⁻¹⁹. In this model, disuse of the limb causes a reduction in gastrocnemius muscle tension, which will initiate a process of protein content degradation with a consequent reduction in the cross-sectional area of the muscle fiber, in addition to a reduction in muscle glycogen reserves, proliferation of intramuscular connective tissue, decreased neuromuscular transmission and compromised force production¹⁷⁻¹⁹. Furthermore, this type of immobilization can result in changes in the strength-length relationship by the position in which the muscle is positioned during immobilization, and according to Shah et al.²⁰, immobilization with the musculature in a shortened position will cause a decrease in the number of sarcomeres. Previous studies reveal that this type of muscle morphological change is more pronounced in the period of two or three weeks after immobilization in a shortened position^{18,19}.

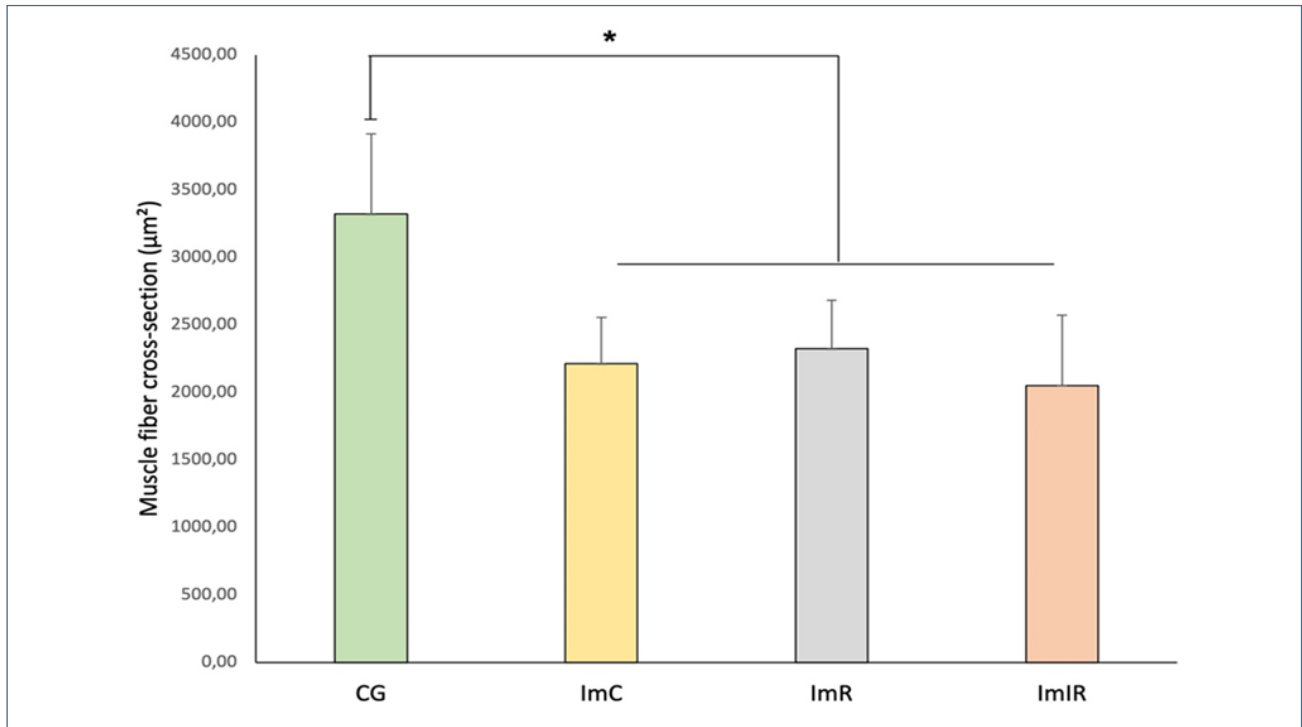


Figure 2: Morphometric analysis of CSA. Basal control (CG) animals were not immobilized and did not receive any type of treatment; immobilized animals with no treatment (ImC); immobilized animals submitted to red laser with a wavelength of 660 nm treatment (ImR); immobilized animals submitted to near-infrared laser with a wavelength of 808 nm treatment (ImIR) (indicated as * $p=0.05$ versus CG).

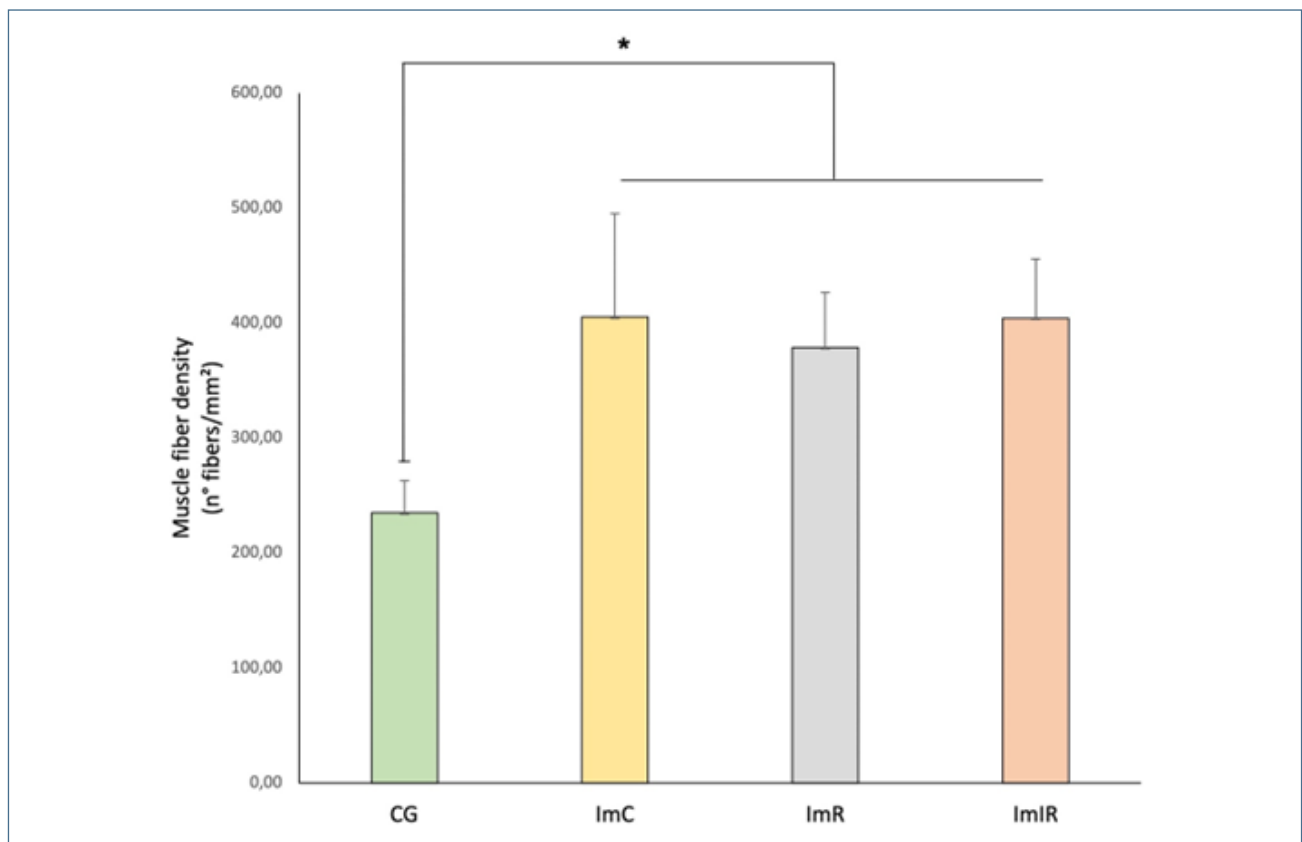


Figure 3: Muscle fiber density. Basal control (CG) animals were not immobilized and did not receive any type of treatment; immobilized animals with no treatment (ImC); immobilized animals submitted to red laser with a wavelength of 660 nm treatment (ImR); immobilized animals submitted to near-infrared laser with a wavelength of 808 nm treatment (ImIR) (indicated as * $p=0.05$ versus CG).

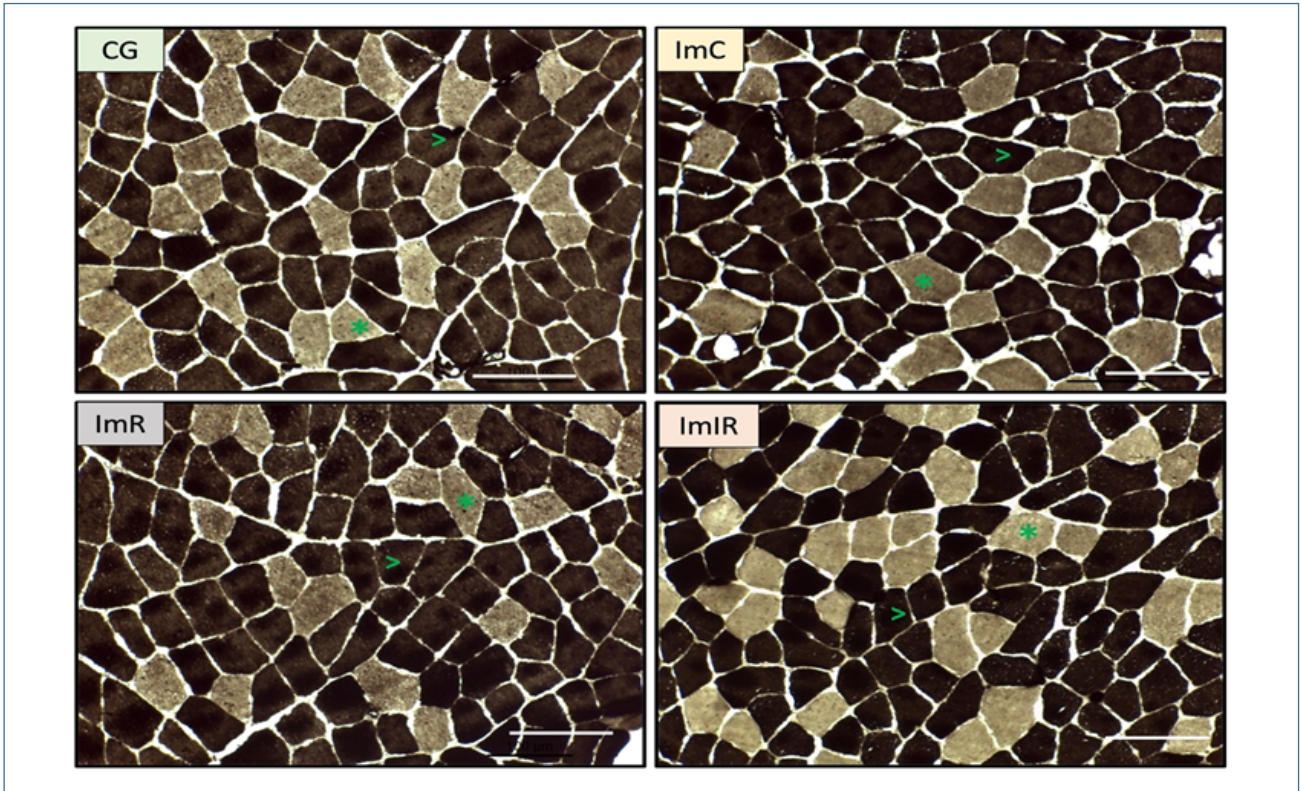


Figure 4: Photomicrographs of ATPase analysis of gastrocnemius muscle cross-sections. Type I fibers (asterisk); Type II fibers (arrowhead); Basal control (CG) animals were not immobilized and did not receive any type of treatment; immobilized animals with no treatment (ImC); immobilized animals submitted to red laser with a wavelength of 660 nm treatment (ImR); immobilized animals submitted to near-infrared laser with a wavelength of 808 nm treatment (ImIR). (ATPase 9.4 staining. Scale bar =100 µm).

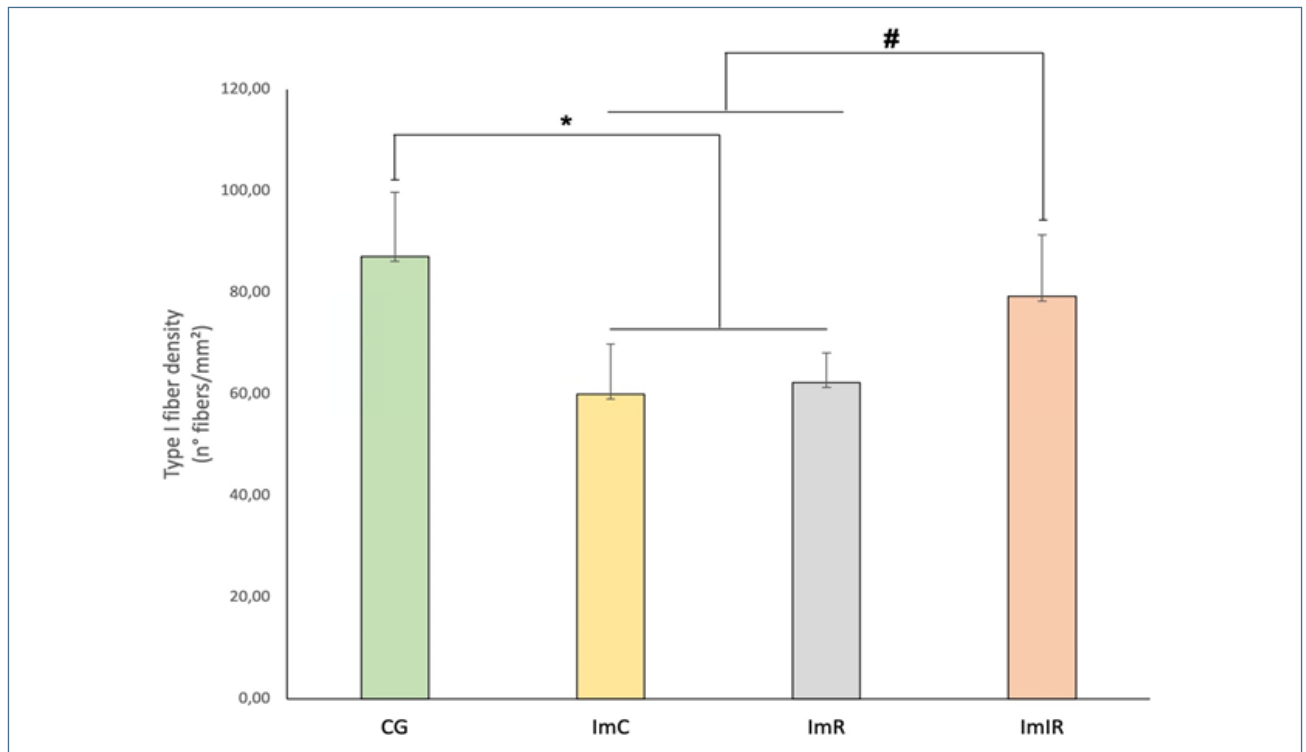


Figure 5: Type I fiber density. Basal control (CG) animals were not immobilized and did not receive any type of treatment; immobilized animals with no treatment (ImC); immobilized animals submitted to red laser with a wavelength of 660 nm treatment (ImR); immobilized animals submitted to near-infrared laser with a wavelength of 808 nm treatment (ImIR) (indicated as * $p=0.05$ versus CG and # versus ImIR).

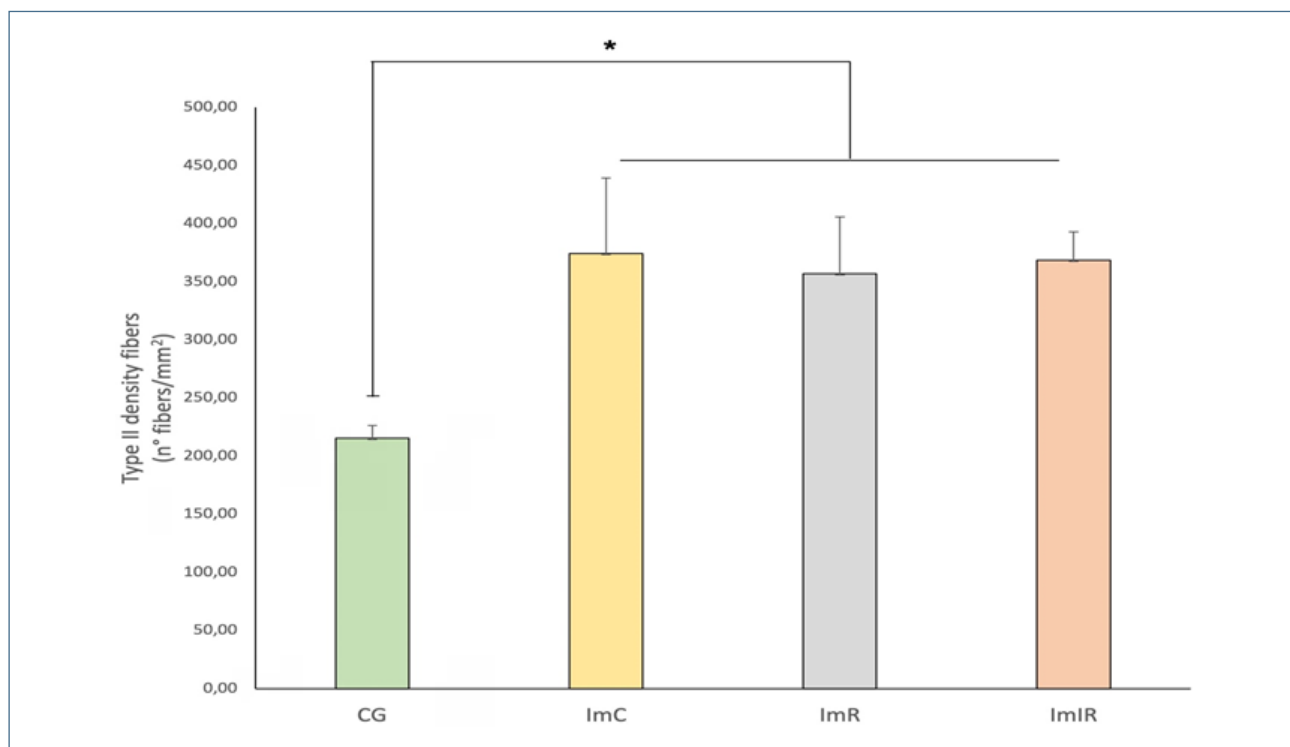


Figure 6: Type II fiber density. Basal control (CG) animals were not immobilized and did not receive any type of treatment; immobilized animals with no treatment (ImC); immobilized animals submitted to red laser with a wavelength of 660 nm treatment (ImR); immobilized animals submitted to near-infrared laser with a wavelength of 808 nm treatment (ImIR) (indicated as * $p=0.05$ versus CG).

On the other hand, some studies show significant muscle adaptations between 1 and 7 days after immobilization^{21,22}.

The histological analysis of the present study is consistent with the morphological findings of the studies, since in animals that were submitted to the joint immobilization model for 5 days, the presence of inflammatory cell infiltrate, muscle fibers with varied shapes can be observed in the analyzed muscles and irregular size, reduced profile and increased density of muscle fibers, in addition to thickening of the intramuscular connective tissue. Evidence shows that in the initial stage of the atrophy process due to immobilization, muscle proteolysis is directly associated with the increase of pro-inflammatory cytokines (especially TNF- α and IL-1 β) that cause the activation of the ubiquitin-proteasome system pathways²³. Furthermore, the proliferation of intramuscular connective tissue is linked to a reduction in active and passive muscle tension, which occurs during immobilization, associated with changes in fibroblast activity that increase the synthesis of intramuscular connective tissue, especially in immobilization by shortening, corroborating with the findings observed in the present study^{19,24} describe an increase in connective tissue density within 2 days after immobilization and suggest that the reduction in muscle mechanical load is linked to the production of growth factors that stimulate collagen synthesis. The same authors describe that the morphological observations related to the increase in the intramuscular connective tissue cause a mechanical barrier

that interferes with the blood flow from the capillaries to the muscle fibers, accentuating the atrophy process.

Interestingly, in the present study, after treatment with laser PBMT applied at two points in the gastrocnemius muscle, the animals presented reduced inflammatory infiltrates and less connective tissue thickening when compared to the ImC. Furthermore, it was also possible to verify that the ImIR animals had less inflammatory infiltrate, less connective tissue thickening, and the presence of regenerating muscle fibers (fibers with a central nucleus) when compared to the ImR.

The application of PBMT on muscle tissue through trophic changes has been the object of intense scientific study in recent years²⁵⁻²⁷. In these studies, the use of PBMT within the ranges intended for visible light and/or near-infrared is observed. Within this context, it is suggested that the main role of PBMT in muscle tissue in the atrophy process is related to the effect that the therapy can modulate the inflammatory process, inhibit the activation of the UPS system, and stimulate the proliferation of satellite cells responsible for myogenesis and formation of new muscle fibers²⁸. Studies in several models show that this therapeutic approach can induce the expression of cell cycle regulatory proteins and activate satellite cells²⁹⁻³¹, stimulating myotube formation³², promoting angiogenesis³³, increasing the number of regenerating fibers and mitochondrial density and activity^{25,31,34}, in addition to improving the organization of regenerated muscle

fibers³⁵. Thus, all these stimuli caused by the action of PBMT in muscle tissue can explain the morphological findings observed in muscles that underwent laser treatment.

Furthermore, the more pronounced effects observed in the present study in the ImIR group may be related to the ability of greater tissue penetration compared to the ImR, which could intensify the transfer of electrons within the cytochrome of a greater number of cells and, consequently, stimulate more nuclear factors responsible for modulating the inflammatory process, stimulating myogenesis and inhibiting pathways related to muscle proteolysis^{28,29}. Muniz et al.³⁶ and Mandelbaum-Livnat et al.³⁷ also describe that the infrared laser provided attenuation of muscle atrophy in experimental studies. Using a disuse-induced muscle atrophy model (pelvic limb suspension), Nakano et al.³¹ demonstrated that the treatment with PBMT caused in the infrared wavelength (830 nm) provided an increase in the diameter of myofibers and the number of capillaries, and significantly increased the proliferation of satellite cells and myofibers of the atrophied muscle. Furthermore, Kou et al.³⁸ reported that PBMT attenuated the progression of muscle atrophy induced by disuse because the therapy increases the proliferation of satellite cells and protects against cellular apoptosis. More recently, Svobodova et al.³⁹ demonstrated that PBMT (808 and 905 nm) resulted in positive effects in the preservation of muscle atrophy induced after spinal cord injury. Furthermore, in a model of muscle atrophy induced after transection of the anterior cruciate ligament, Assis et al.⁴⁰, verified that PBMT (808 nm) was able to significantly increase the muscle section area, decrease the muscle fiber density and the expression of atrogin-1 and Murf-1, proteins responsible for the proteolysis of the muscle fiber.

Regarding the smaller amount of connective tissue observed in the present study in animals undergoing PBMT, with emphasis on the IR, it can be inferred that the therapy prevented the deposition of fibrous tissue, favoring the recovery of skeletal muscle. As mentioned above, excessive collagen deposition between capillaries and myofiber membranes reduces the nutritional support of muscle fibers, impairing muscle regeneration. Assis et al.¹² verified that laser PBMT at an infrared wavelength exerted a positive biological effect on regenerating muscle tissue since it reduced the expression of TGF- β with a consequent reduction in local collagen accumulation, preventing the deposition of fibrous tissue and favoring skeletal muscle recovery¹².

Additionally, it is known that periods of muscle disuse promote marked mitochondrial alterations that contribute to the impairment of muscle fiber metabolism². It is reported that oxidative muscle fibers (type I) are the most vulnerable to muscle atrophy when compared to glycolytic fibers (type II)^{1,2}. In the present study, we observed a reduction in type I fibers in the immobilized groups and an increase in type II

fibers, demonstrating that the immobilization caused a predominance of glycolytic fibers. Interestingly, in the muscle irradiated with PBMT, there was a greater number of oxidative fibers when compared to the other immobilized groups. Previous studies suggest that PBMT proves to be effective in reestablishing the bioenergetic pathways of muscle metabolism, increasing ATP synthesis, and reducing the end products of oxidative stress¹². Furthermore, there is evidence that irradiation promotes the proliferation and fusion of mitochondria, increasing mitochondrial density and size in tissue¹²⁻¹⁴. Thus, it is believed that these effects may have positive repercussions during the rehabilitation of atrophied muscle since light may have provided an energy increase in the muscle fiber, thus maintaining the number of oxidative muscle fibers observed in the present study.

Based on the results observed in the present study, it can be observed that the period of 5 days of immobilization was sufficient to cause significant morphological changes characteristic of muscle atrophy. The treatment immediately after the removal of the immobilization, using PBMT with red laser and infrared, was able to induce an adequate tissue response to modulate the signs of muscle atrophy, with these results being more evident with the infrared.

Thus, the present study provides important information about the effect of laser PBMT as an adjunct to the treatment of muscle atrophy, suggesting the choice of therapy in the early rehabilitation of muscles submitted to short-term immobilization.

Yet, as part of an ongoing effort to mobilize clinical tools (non-invasive, relatively inexpensive, and with no reported side effects) with the potential to attenuate muscle atrophy due to immobility, the present study offers compelling reasons to explore the potential effects of infrared PBMT as prevention complications associated with atrophy. However, it is necessary to investigate, through experimental and clinical studies, controlled and randomized, to validate whether this and other light spectra could be beneficial in the prevention and/or attenuation of muscle atrophy.

Conclusion

In conclusion, the findings of the present study suggest that red and infrared laser PBMT were able to promote changes in the morphology of the gastrocnemius muscle submitted to atrophy in an experimental immobilization model, reducing the inflammatory infiltrate and the formation of intramuscular connective tissue. However, infrared laser PBMT promoted more evident positive effects by increasing regenerating muscle fibers and the number of oxidative fibers. This type of experimental evidence is necessary for the design of other clinical trials involving the use of PBMT in disorders that affect the musculoskeletal system.

REFERENCES

1. Bodine SC, Baehr LM. Skeletal muscle atrophy and the E3 ubiquitin ligases MuRF1 and MAFbx/atrogin-1. *Am J Physiol Endocrinol Metab.* 2014;307(6):E469-84. <https://doi.org/10.1152/ajpendo.00204.2014>
2. Lee JH, Jun HS. Role of Myokines in Regulating Skeletal Muscle Mass and Function. *Front Physiol.* 2019;10:42. <https://doi.org/10.3389/fphys.2019.00042>
3. Rosa-Caldwell ME, Greene NP. Muscle metabolism and atrophy let's talk about sex. *Biol Sex Differ.* 2019;10(1):43. <https://doi.org/10.1186/s13293-019-0257-3>
4. Morley JE, Kalantar-Zadeh K, Anker SD. COVID-19: a major cause of cachexia and sarcopenia? *J Cachexia Sarcopenia Muscle.* 2020;11(4):863-65. <https://doi.org/10.1002/jcsm.12589>
5. March L, Smith EU, Hoy DG, Cross MJ, Sanchez-Riera L, Blyth F, et al. Burden of disability due to musculoskeletal (MSK) disorders. *Best Pract Res Clin Rheumatol.* 2014;28(3):353-66. <https://doi.org/10.1016/j.berh.2014.08.002>
6. Beaudart C, Biver E, Bruyère O, Cooper C, Al-Daghri N, Reginster JY, et al. Quality of life assessment in musculo-skeletal health. *Aging Clin Exp Res.* 2018;30(5):413-18. <https://doi.org/10.1007/s40520-017-0794-8>
7. Gruet M, Troosters T, Verges S. Peripheral muscle abnormalities in cystic fibrosis: Etiology, clinical implications and response to therapeutic interventions. *J Cyst Fibros.* 2017;16(5):538-52. <https://doi.org/10.1016/j.jcf.2017.02.007>
8. Lee JH, Jun HS. Role of myokines in regulating skeletal muscle mass and function. *Front Physiol.* 2019; 10:42. <https://doi.org/10.3389/fphys.2019.00042>
9. You JS, Anderson GB, Dooley MS, Hornberger TA. The role of mTOR signaling in the regulation of protein synthesis and muscle mass during immobilization in mice. *Dis Model Mech.* 2015;8(9):1059-69. <https://doi.org/10.1242/dmm.019414>
10. Chung H, Dai T, Sharma SK, Huang YY, Carroll JD, Hamblin MR. The nuts and bolts of low-level laser (light) therapy. *Ann Biomed Eng.* 2012;40(2):516-33. <https://doi.org/10.1111/apha.12532>
11. Freitas LF, Hamblin MR. Proposed mechanisms of photobiomodulation or low-level light therapy. *IEEE J Sel Top Quantum Electron.* 2016;22(3):7000417. <https://doi.org/10.1109/JSTQE.2016.2561201>
12. Assis L, Moretti AI, Abrahão TB, Souza HP, Hamblin MR, Parizotto NA. Low-level laser therapy (808 nm) contributes to muscle regeneration and prevents fibrosis in rat tibialis anterior muscle after cryolesion. *Lasers Med Sci.* 2013;28(3):947-55. <https://doi.org/10.1007/s10103-012-1183-3>
13. Ferraresi C, Hamblin MR, Parizotto NA. Low-level laser (light) therapy (LLL) on muscle tissue: performance, fatigue, and repair benefited by the power of light. *Photonics Lasers Med.* 2012;1(4):267-86. <https://doi.org/10.1515/plm-2012-0032>
14. Lakyová L, Toporcer T, Tomečková V, Sábó J, Radoňák J. Low-level laser therapy for protection against skeletal muscle damage after ischemia-reperfusion injury in rat hindlimbs. *Lasers Surg Med.* 2010;42(9):665-72. <https://doi.org/10.1002/lsm.20967>
15. Quintana HT, Baptista VIA, Lazzarin MC, Antunes HKM, Le Sueur-Maluf L, Oliveira CAM, et al. Insulin modulates myogenesis and muscle atrophy resulting from skin scald burn in young male rats. *J Surg Res.* 2021;257:56-68. <https://doi.org/10.1016/j.jss.2020.07.040>
16. Dubowitz V, Sewry CA, Fitzsimons RB. Muscle biopsy a practical approach. 2nd ed. London: Bailliere Tindall, 1985.
17. Zhang P, Chen X, Fan M. Signaling mechanisms involved in disuse muscle atrophy. *Med Hypotheses.* 2007;69(2):310-21. <https://doi.org/10.1016/j.mehy.2006.11.043>
18. Gomes AR, Coutinho EL, França CN, Polonio J, Salvini TF. Effect of one stretch a week applied to the immobilized soleus muscle on rat muscle fiber morphology. *Braz J Med Biol Res.* 2004;37(10):1473-80. <https://doi.org/10.1590/s0100-879x2004001000005>
19. Williams PE, Goldspink G. Changes in sarcomere length and physiological properties in immobilized muscle. *J Anat.* 1978;127(Pt 3):459-68.
20. Shah SB, Peters D, Jordan KA, Milner DJ, Fridén J, Capetanaki Y, et al. Sarcomere number regulation maintained after immobilization in desmin-null mouse skeletal muscle. *J Exp Biol.* 2001;204(Pt 10):1703-10.
21. Järvinen MJ, Einola SA, Virtanen EO. Effect of the position of immobilization upon the tensile properties of the rat gastrocnemius muscle. *Arch Phys Med Rehabil.* 1992;73(3):253-7.
22. Ahtikoski AM, Koskinen SO, Virtanen P, Kovanen V, Risteli J, Takala TE. Synthesis and degradation of type IV collagen in rat skeletal muscle during immobilization in shortened and lengthened positions. *Acta Physiol Scand.* 2003;177(4):473-81. <https://doi.org/10.1046/j.1365-201X.2003.01061.x>
23. Wall BT, Dirks ML, Snijders T, Senden JM, Dolmans J, van Loon LJ. Substantial skeletal muscle loss occurs during only 5 days of disuse. *Acta Physiol (Oxf).* 2014;210(3):600-11. <https://doi.org/10.1111/apha.12190>
24. Järvinen TA, Józsa L, Kannus P, Järvinen TL, Järvinen M. Organization and distribution of intramuscular connective tissue in normal and immobilized skeletal muscles. An immunohistochemical, polarization and scanning electron microscopic study. *J Muscle Res Cell Motil.* 2002;23(3):245-54. <https://doi.org/10.1023/a:1020904518336>
25. Amaral AC, Parizotto NA, Salvini TF. Dose-dependency of low-energy HeNe laser effect in regeneration of skeletal muscle in mice. *Lasers Med Sci.* 2001;16(1):44-51. <https://doi.org/10.1007/pl00011336>
26. Mesquita-Ferrari RA, Martins MD, Silva JA Jr, Silva TD, Piovesan RF, Pavesi VC, et al. Effects of low-level laser therapy on expression of TNF- α and TGF- β in skeletal muscle during the repair process. *Lasers Med Sci.* 2011;26(3):335-40. <https://doi.org/10.1007/s10103-010-0850-5>
27. Ramos L, Leal Junior EC, Pallotta RC, Frigo L, Marcos RL, Carvalho MH, et al. Infrared (810 nm) low-level laser therapy in experimental model of strain-induced skeletal muscle injury in rats: effects on functional outcomes. *Photochem Photobiol.* 2012;88(1):154-60. <https://doi.org/10.1111/j.1751-1097.2011.01030.x>
28. Gonçalves SR, Tim CR, Martignago CCS, Silva MCP, Anaruma CA, Garcia LA. Potential of photobiomodulation therapy in the treatment of skeletal muscle atrophy. *Res Soc Dev.* 2021;10(1):e931018527. <https://doi.org/10.33448/rsd-v10i1.8527>
29. Ben-Dov N, Shefer G, Irintchev A, Wernig A, Oron U, Halevy O. Low-energy laser irradiation affects satellite cell proliferation and differentiation in vitro. *Biochim Biophys Acta.* 1999;1448(3):372-80. [https://doi.org/10.1016/s0167-4889\(98\)00147-5](https://doi.org/10.1016/s0167-4889(98)00147-5)
30. Shefer G, Oron U, Irintchev A, Wernig A, Halevy O. Skeletal muscle cell activation by low-energy laser irradiation: a role for the MAPK/ERK pathway. *J Cell Physiol.* 2001;187(1):73-80. [https://doi.org/10.1002/1097-4652\(2001\)9999:9999::AID-JCP1053>3.0.CO;2-9](https://doi.org/10.1002/1097-4652(2001)9999:9999::AID-JCP1053>3.0.CO;2-9)

31. Nakano J, Kataoka H, Sakamoto J, Origuchi T, Okita M, Yoshimura T. Low-level laser irradiation promotes the recovery of atrophied gastrocnemius skeletal muscle in rats. *Exp Physiol*. 2009;94(9):1005-15.
<https://doi.org/10.1113/expphysiol.2009.047738>
32. Bibikova A, Belkin V, Oron U. Enhancement of angiogenesis in regenerating gastrocnemius muscle of the toad (*Bufo viridis*) by low-energy laser irradiation. *Anat Embryol (Berl)*. 1994;190(6):597-602.
<https://doi.org/10.1007/BF00190110>
33. Iyomasa DM, Garavelo I, Iyomasa MM, Watanabe IS, Issa JP. Ultrastructural analysis of the low-level laser therapy effects on the lesioned anterior tibial muscle in the gerbil. *Micron*. 2009;40(4):413-8.
<https://doi.org/10.1016/j.micron.2009.02.002>
34. Silveira PC, Silva LA, Fraga DB, Freitas TP, Streck EL, Pinho R. Evaluation of mitochondrial respiratory chain activity in muscle healing by low-level laser therapy. *J Photochem Photobiol B*. 2009;95(2):89-92.
<https://doi.org/10.1016/j.jphotobiol.2009.01.004>
35. Cressoni MDC, Giusti HHKD, Casarotto RA, Anaruma CA. The effects of a 785-nm AlGalnP laser on the regeneration of rat anterior tibialis muscle after surgically induced injury. *Photomed Laser Surg*. 2008;26(5):461-6.
<https://doi.org/10.1089/pho.2007.2150>
36. Muniz KL, Dias FJ, Coutinho-Netto J, Calzani RA, Iyomasa MM, Sousa LG, et al. Properties of the tibialis anterior muscle after treatment with laser therapy and natural latex protein following sciatic nerve crush. *Muscle Nerve*. 2015;52(5):869-75.
<https://doi.org/10.1002/mus.24602>
37. Mandelbaum-Livnat MM, Almog M, Nissan M, Loeb E, Shapira Y, Rochkind S. Photobiomodulation Triple Treatment in Peripheral Nerve Injury: Nerve and Muscle Response. *Photomed Laser Surg*. 2016;34(12):638-45.
<https://doi.org/10.1089/pho.2016.4095>
38. Kou YT, Liu HT, Hou CY, Lin CY, Tsai CM, Chang H. A transient protective effect of low-level laser irradiation against disuse-induced atrophy of rats. *Lasers Med Sci*. 2019;34(9):1829-39.
<https://doi.org/10.1007/s10103-019-02778-5>
39. Svobodova B, Kloudova A, Ruzicka J, Kajtmanova L, Navratil L, Sedlacek R, et al. The effect of 808 nm and 905 nm wavelength light on recovery after spinal cord injury. *Sci Rep*. 2019;9(1):7660.
<https://doi.org/10.1038/s41598-019-44141-2>
40. Assis L, Almeida T, Milares LP, Passos N, Araújo B, Bublitz C, et al. Musculoskeletal atrophy in an experimental model of knee osteoarthritis: the effects of exercise training and low-level laser therapy. *Am J Phys Med Rehabil*. 2015;94(8):609-16.
<https://doi.org/10.1097/PHM.0000000000000219>